Supplementary information for

Aerobic Degradation of Sulfadiazine by *Arthrobacter* spp.: Kinetics, Pathways and Genomic Characterization

Yu Deng[†], Yanping Mao[†], Bing Li[†], Chao Yang[†] and Tong Zhang[†*]

[†]Environmental Biotechnology Laboratory, Department of Civil Engineering, The University of Hong Kong, Pokfulam Road, Hong Kong

[*]Corresponding author, +852-28578551; fax:+852-25595337; zhangt@hkucc.hku.hk

CONTENTS

LIST OF TABLES

LIST OF FIGURES

REFERENCES

Materials and Methods

Chemicals and strains. Sulfadiazine (99% of purity), 2-aminopyrimidine (97% of purity) and 2-amino-4,6-dihydroxypyrimidine (98% of purity) were obtained from Sigma-Aldrich. And sulfanilamide of analytical purity was purchased from BDH Chemicals. 2-amino-4-hydroxypyrimidine of 95% purity was purchased from Acros and 2-amino-5-hydroxypyrimidine of 98% purity was purchased from TCI. Five pure cultures used in this study including *Arthrobacter ureafaciens* strain NC (DSM 20126), *Arthrobacter histidinolovorans* strain DSM 20115, *Arthrobacter nicotinovorans* strain DSM 420, *Arthrobacter nitroguajacolicus* strain G2-1 (DSM 15232) and *Arthrobacter aurescens* strain DSM 20116 were all obtained from DSMZ (German Collection of Microorganisms and Cell Cultures, Germany).

Culture enrichment. SDZ-degrading consortium was enriched by a two-stage process: 400 mL actived sludge from a local municipal wastewater treatment plant were initially used as inoculum in two 500 mL reactors, SDZ Enriched 1 and SDZ Enriched 2, followed by sequential drawing and refilling with 100 mL defined mineral salts medium supplemented with 0.3 g/L sodium acetate and 10 mg/L SDZ every 3 days. When efficient SDZ degradation was observed, the liquid in each reactor was replaced with the same volume of MSM containing 50 mg/L SDZ as the sole organic carbon source.

PCR. The universal bacterial primers 27F (5'-AGAGTTTGATCMTGGCTCAG-3') 1492R (5'-TACGGYTACCTTGTTACGACTT-3') were used for the PCR assays. The 50 μL PCR reaction mixture contained 25 μL of 2 × Premix Taq TM (TaKaRa, Japan), 21 μL of nuclease-free water, 1μL of each primer and 2 μL of sample DNA. The thermocycling procedures started with a step of 95 ℃ for 5 min, followed by 30 cycles including 95 ℃ for 1 min, 55 ℃ for 0.5 min and 72 ℃ for 2 min. The final extension step was set to 72 ℃ for 5 min.

Scanning electron microscopy. Isolates grown to mid-log phase were collected by centrifugation and washed three times with PBS (50 mM, pH=7). Afterwards, cells were fixed overnight in 2.5% glutaraldehyde (v/v) in PBS (50 mM, pH=7). The fixed cells were washed three times again with the same agent, and were dehydrated in an up-grading series of ethanol (25, 50, 75, 90, 95, 98, 99, and 100%), with 30 min interval for each concentration. The dried cells were then observed by a Hitachi S-4800 FEG Scanning Electron Microscope.

Incubation experiment and treatments. In order to obtain SDZ-induced and non-induced cells, single colony of isolates was initially inoculated in 100 mL flasks containing 20 mL MSM supplemented either with SDZ (50 mg/L) or glucose (2 g/L) as the sole carbon source, respectively. After being cultivated at 37 ℃ on a rotary shaker (200 rpm) for certain days, the capacity of induced and non-induced cells to degrade SDZ were tested in resting state in PBS (50 mM, pH=7) and an initial OD_{595} of 2.0. For growing and resting cells, single colony was initially seeded into a 20 mL LB liquid medium amended with 50 mg/L SDZ and cultured till mid-lag phase. Cells were then harvested by centrifugation at 4000 rpm for 5 min, and were washed three times using PBS (50 mM, pH=7) before the experiments, and finally re-suspended in MSM containing 50 mg/L SDZ for growing cells and PBS (50 mM, pH=7) containing 50 mg/L SDZ for resting cells. For the TOC measurements, 20 mL mixed liquid was withdrawn and filtrated with 0.45 μm nylon filter.

Lineage-specific markers. The lineage-specific markers for whole genome phylogenetic analyses inferred CheckM includes:

TIGR01173, PF11296.3, PF00308.13, PF12029.3, PF01619.13,
PF01761.15, PF00318.15, PF01189.12, PF12502.3, PF00297.17,
PF01939.11, PF03320.8, PF01195.14, PF00164.20, PF00453.13,
PF07516.8, PF11898.3, TIGR00409, PF02773.11, PF08328.6,
PF01784.13, PF00166.16, PF12089.3, PF02222.17, PF00687.16,
PF00162.14, TIGR00966, TIGR00049, PF00252.13, PF01795.14,
PF06574.7, PF02601.10, PF03143.12, PF03946.9, PF02153.12,
PF00119.15, PF01196.14, PF01746.16, PF00988.17, TIGR00112,
PF01715.12, PF02401.13, PF02527.10, TIGR01245, PF01807.15,
PF02645.11, PF01379.15, PF00490.16, PF01351.13, PF00189.15,
PF13292.1, PF04997.7, PF00889.14, TIGR02692, PF00623.15,
PF12327.3, PF11987.3, PF00218.16, PF00410.14, PF00177.16,
PF02545.9, PF01653.13, TIGR01499, TIGR00498, TIGR01951,
PF02130.12, TIGR00382, PF00303.14, PF04560.15, PF04417.7,
PF02075.12, TIGR00152, PF00347.18, TIGR00326, PF00237.14,
TIGR00234, TIGR00185, PF01641.13, PF00673.16, TIGR00214,
TIGR00624, TIGR01082, TIGR01083, PF03993.7, PF04998.12,
PF02390.12, PF03668.10, PF01220.14, PF01450.14, TIGR03448,
PF02934.10, PF03602.10, PF04452.9, PF00238.14, TIGR00751,
PF00958.17, PF04127.10, TIGR03723, PF08436.7, PF01207.12,
PF00861.17, TIGR00878, TIGR02075, PF00572.13, PF01431.16,

TIGR00010, PF12282.3, PF01043.15, PF00438.15, PF01245.15, PF01071.14, PF11361.3, PF00380.14, TIGR00329, PF02381.13, TIGR02127, PF10150.4, PF01933.13, TIGR01356, PF02787.14, PF01625.16, PF00186.14, TIGR03594, TIGR00611, TIGR00389, TIGR00717, TIGR00419, PF06418.9, PF04461.8, PF07479.9, TIGR01745, PF01474.11, PF04551.9, PF10698.4, PF00573.17, PF11241.3, PF06071.8, TIGR00539, PF03883.9, PF01678.14, TIGR03543, PF01259.13, PF06421.7, PF01808.13, TIGR00173, TIGR00093, PF00411.14, TIGR01019.

Results and Discussion

Morphologic Characterization of the Isolates. Members of the genus *Arthrobacter* are reported to be asporogenous, aerobic gram-positive bacilli[1] characterized with the rod-coccus growth cycle[2] and the V-form arrangement of cells.[3] Coccoid cells were expected to be formed in stationary phase based on the rod-coccus transformations.[4] The SEM observations of strains D2 and D4 showed that both isolates grown to mid-log phase were rod shape with transient branches in different lengths. A majority of the observed cells of strains D2 and D4 were homogeneously appeared in several V-forms (Figure S15). In the present study, these V-forms of strains D2 and D4 may arise by the germination of coccoid or rod buds or the unusual cell division known as "snapping division" (Figure S14d). Snapping division represents a pattern of post-fission movement particular to certain strains of bacilli and therefore has been proposed as a possible taxonomic criterion.[5] Arrows in Figure S15a and b indicate the externally visible ridges which may form during the cell elongation. The ridge structures were relatively smooth in appearance compared with artificial cracks due to sample preparation (Figure S15c). Multiple ridges can be accumulated on a single cell, which was indicative of active divisions.[6] Apparently, positions of multiple ridges on a single cell were not equidistantly displayed, implying that the daughter cell may undergo asymmetrical elongation after the division of germ cell.

Degradation Products and Pathways in Pure Culture. The corresponding ions for peak at 3.51 min were at *m/z* 130, 176 and 278. However, the structures of two ions (*m/z* 130 and 278) eluting in this peak were still uncertain by the approach developed in this work. As for the ion at *m/z* 176, three distinct MS/MS fragments were identified at *m/z* 77, 103 and 130, indicating that this product would correspond to pyrimidin-2-ylsulfamic acid. As for the peak at a retention time of 2.45 min, base ions at *m/z* 136 and 298 were recorded. Considering the 162 Da difference between these

two ions, the ion at *m/z* 298 could correspond to the glucosidation of the ion at *m/z* 136.[7] Based on the literature, the glucosidation likely occurred at the electron-rich nucleophilic positions of sulfonamide antibiotics, which was reported as one of the major transformation reactions for sulfonamides in natural environmental processes like human metabolism[8] and biodegradation by microorganisms.[9, 10]

Table S1. Composition of the defined mineral source medium

Substrate	Nutrients	Concentration
Culture medium	Na_2HPO_4	6.81 g/L
	$MgSO_4•H_2O$	0.112 g/L
	KH_2PO_4	0.675 g/L
	$CaCl_2$	0.015 g/L
	NH_4Cl	20.4 mg/L
Trace elements	$FeSO_4•7H_2O$	1 mg/L
	$MnSO_4•H_2O$	1 mg/L
	$CuCl•2H_2O$	0.25 mg/L
	$Na_2MoO_4•2H_2O$	0.25 mg/L

Table S2. 16S rRNA similarity between two isolates and two enriched consortia

SDZ Enriched 1	Isolates	Similarity (%)	SDZ Enriched 1	Isolates	Similarity (%)
SDZEnriched1-4	D2	97.47	SDZEnriched2-18	D4	98.38
SDZEnriched1-32	D2	97.44	SDZEnriched2-32	D4	98.24
SDZEnriched1-15	D2	97.4	SDZEnriched2-5	D4	98.1
SDZEnriched1-16	D2	97.34	SDZEnriched2-6	D2	97.57
SDZEnriched1-7	D2	97.33	SDZEnriched2-2	D2	97.38
SDZEnriched1-13	D2	97.32	SDZEnriched2-12	D2	97.38
SDZEnriched1-36	D2	97.31	SDZEnriched2-16	D2	97.38
SDZEnriched1-26	D2	97.26	SDZEnriched2-10	D2	97.37
SDZEnriched1-40	D2	97.03	SDZEnriched2-29	D2	97.35
SDZEnriched1-32	D4	96.09	SDZEnriched2-26	D2	97.32
SDZEnriched1-4	D4	96.06	SDZEnriched2-20	D2	97.2
SDZEnriched1-15	D4	95.95	SDZEnriched2-17	D2	97.08
SDZEnriched1-16	D4	95.94	SDZEnriched2-7	D2	96.98
SDZEnriched1-7	D4	95.92	SDZEnriched2-18	D2	96.66
SDZEnriched1-13	D4	95.91	SDZEnriched2-32	D2	96.66
SDZEnriched1-26	D4	95.82	SDZEnriched2-39	D2	96.32
SDZEnriched1-36	D4	95.82	SDZEnriched2-5	D2	96.26
SDZEnriched1-40	D4	95.48	SDZEnriched2-6	D4	96.21
SDZEnriched1-31	D4	82.3	SDZEnriched2-29	D4	95.96
SDZEnriched1-34	D4	82.11	SDZEnriched2-2	D4	95.92
SDZEnriched1-6	D4	81.75	SDZEnriched2-12	D4	95.92
SDZEnriched1-1	D2	81.61	SDZEnriched2-16	D4	95.92
SDZEnriched1-28	D2	81.61	SDZEnriched2-10	D4	95.9
SDZEnriched1-33	D2	81.61	SDZEnriched2-26	D4	95.83

SDZEnriched1-8	D2	81.32	SDZEnriched2-20	D4	95.65
SDZEnriched1-27	D2	81.32	SDZEnriched2-17	D4	95.63
SDZEnriched1-34	D2	81.16	SDZEnriched2-7	D4	95.4
SDZEnriched1-6	D2	80.87	SDZEnriched2-39	D4	94.53
SDZEnriched1-38	D2	80.77	SDZEnriched2-9	D4	82.11
SDZEnriched1-31	D2	80.67	SDZEnriched2-9	D2	80.87
SDZEnriched1-1	D4	80.06	SDZEnriched2-25	D2	80.63
SDZEnriched1-27	D4	80.06	SDZEnriched2-34	D4	80.35
SDZEnriched1-28	D4	80.06	SDZEnriched2-34	D2	79.56
SDZEnriched1-33	D4	80.06	SDZEnriched2-15	D2	79.46
SDZEnriched1-30	D2	79.88	SDZEnriched2-8	D4	79.25
SDZEnriched1-8	D4	79.76	SDZEnriched2-21	D4	79.1
SDZEnriched1-30	D4	79.45	SDZEnriched2-8	D2	78.94
SDZEnriched1-14	D2	79.26	SDZEnriched2-4	D4	78.76
SDZEnriched1-18	D4	79.26	SDZEnriched2-3	D4	78.63
SDZEnriched1-9	D2	79.21	SDZEnriched2-4	D2	78.5
SDZEnriched1-17	D2	79.21	SDZEnriched2-15	D4	78.37
SDZEnriched1-23	D4	78.83	SDZEnriched2-21	D2	78.25
SDZEnriched1-25	D2	78.83	SDZEnriched2-37	D4	78.01
SDZEnriched1-29	D2	78.56	SDZEnriched2-37	D2	77.39
SDZEnriched1-38	D4	78.55	SDZEnriched2-35	D2	77.37
SDZEnriched1-21	D4	78.28	SDZEnriched2-24	D4	77.22
SDZEnriched1-14	D4	78.17	SDZEnriched2-40	D4	77.21
SDZEnriched1-9	D4	78.14	SDZEnriched2-36	D4	76.99
SDZEnriched1-17	D4	78.14	SDZEnriched2-35	D4	76.96
SDZEnriched1-21	D2	78.07	SDZEnriched2-31	D4	76.38
SDZEnriched1-23	D2	78.07	SDZEnriched2-28	D4	76.36
SDZEnriched1-12	D2	78.01	SDZEnriched2-14	D4	75.89
SDZEnriched1-18	D2	78.01	SDZEnriched2-27	D2	75.04
SDZEnriched1-12	D4	77.76	SDZEnriched2-27	D4	74.69
SDZEnriched1-25	D4	77.76	SDZEnriched2-1	D2	79.18
SDZEnriched1-10	D2	77.69	SDZEnriched2-1	D4	78.01
SDZEnriched1-19	D2	77.46			
SDZEnriched1-24	D2	77.16			
SDZEnriched1-19	D4	77.1			
SDZEnriched1-22	D4	77.04			
SDZEnriched1-24	D4	76.73			
SDZEnriched1-3	D4	76.7			

Table S3. Similarity of 16S rRNA gene for isolates D2, D4 and their closely related taxa based on BLAST analysis against NCBI database

Organism	**Strain designation**	D2	D4
Arthrobacter sp.	D2		
Arthrobacter sp.	D4	99.9	
Arthrobacter ureafaciens	NC	99.6	99.5
Arthrobacter nicotinovorans	DSM 420	98.4	98.3
Arthrobacter histidinolovorans	DSM 20115	98.0	98.0
Corynebacterium ilicis	ICMP 2608	97.7	97.6
Arthrobacter aurescens	TC1	97.4	97.3
Arthrobacter nitroguajacolicus	G2-1	97.4	97.3
Arthrobacter aurescens	DSM 20116	97.3	97.3

Table S4. Biodegradation of SDZ by induced and non-induced cells of D2 and D4

Isolate	**Non-induced cells**			**SDZ induced cells**		
	Time (h)	SDZ (mg/L)	2-AP (mg/L)	Time (h)	SDZ (mg/L)	2-AP (mg/L)
D2	0	634	0	0	652	0
	48	0	212	48	0	207
D4	0	685	0	0	711	0
	48	500	107	48	0	190

Table S5. Screening of putative biodegradation products by SIR and MRM detection (see total chromatographic profile of the putative biodegradtion products generated from full-scan MS mode in Figure S4)

Putative products *m/z*	**Retention time (min)**	**Determined ion (m/z)**	**False positives subtraction**			
			MS/MS spectrum extraction[a]	**Low intensity noise[b]**	**Random noise during detection[c]**	**Noise identified in samples before SDZ reduction[d]**
***m/z* 1 : 112-0.47min**	**0.47**	**112**	**Yes**	**No**	**No**	**No**
***m/z* 2: 128**		**128**	**Yes**	**No**	**No**	**No**
***m/z* 3: 130-0.47min**		**130**	**Yes**	**No**	**No**	**No**
***m/z* 4: 96**	**0.51**	**96**	**Yes**	**No**	**No**	**No**
***m/z* 5: 87**	**0.67**	**87**	**Yes**	**No**	**No**	**No**
***m/z* 6: 173**		**173**	**Yes**	**No**	**No**	**No**
***m/z* 7: 136**	**2.45**	**136**	**Yes**	**No**	**No**	**No**
***m/z* 8: 298**		**298**	**Yes**	**No**	**No**	**No**
***m/z* 9: 130-3.51min**	**3.51**	**130**	**Yes**	**No**	**No**	**No**
***m/z* 10: 176**		**176**	**Yes**	**No**	**No**	**No**
***m/z* 11: 278**		**278**	**Yes**	**No**	**No**	**No**
***m/z* 12: 243**	**3.94**	**243**	**Yes**	**No**	**No**	**No**
m/z 13: 70-0.46min	0.46	70	NA[e]	No	No	No
m/z 14: 90	0.46	90	NA	No	No	No
m/z 15: 164	0.58	164	NA	No	No	No
m/z 16: 198-0.6min	0.60	198	NA	No	No	No
m/z 17: 88-0.73	0.73	88	NA	No	No	No

m/z 18: 70-0.90min	0.9	70	NA	No	No	No
m/z 19: 198-3.83min	3.51	198	NA	No	No	No
m/z 20: 137	0.47	137	No	Yes	No	No
m/z 21: 88-0.49min	0.47	88	No	Yes	No	No
m/z 22: 153	0.51	153	No	Yes	No	No
m/z 23: 202	0.51	202	No	Yes	No	No
m/z 24: 218	4.10	218	No	No	Yes	No
m/z 25: 246	4.97	246	No	No	Yes	No
m/z 26: 274	5.57	274	No	No	Yes	No
m/z 27: 112-0.98min	0.98	112	No	No	No	Yes
m/z 28: 181-0.98min	0.98	181	No	No	No	Yes

[a]MS/MS spectra extraction was conducted by applying different CE values (10-45 eV) to each plausible single ion using Daughter Scan. 7 ions (*m/z* 13-19) were excluded because their MS/MS spectra were unable to be extracted. This is likely to be caused by the low signal responses for their detection in all samples. [b]After the quantitative assessments by MRM, 4 false positives (Mass 20-23) were rejected as low intensity noise taking into account the S/N ratio of 10 as the lower limit of MRM quantification. [c]By manually checking the time courses of chromatographic peaks for the putative ions, 3 ions at *m/z* 218, 246 and 274 were only detected in one single sample (t=36h for D2 and t=72 h for D4) during 144 h incubation. These 3 ions were the false positives which were attributed to the random detection noises during sample acquisition. [d]The peak appeared at a retention time of 0.98 min in the t=6 day sample was also present in the samples before the SDZ reduction, with comparable intensity (as high as74% for *m/z* 112 before the SDZ reduction sample compared with its highest intensity, and for m/z 181, its highest intensity was recorded in the sample before the SDZ reduction) and same base ions of *m/z* 112 and 181. Therefore, these two ions were identified as noise. [e]NA: Not available.

Table S6. Detail information for 40 genes located on D2 plasmid

No.	D2 locus tag	Contig	Annotation
1	A5N17_17250	D2_contig_29_1	integrase
2	A5N17_17255	D2_contig_29_2	Cro/Cl family transcriptional regulator
3	A5N17_17260	D2_contig_29_3	Fis family transcriptional regulator
4	A5N17_17265	D2_contig_29_4	hypotheticalprotein
5	A5N17_17270	D2_contig_29_5	histidine kinase
6	A5N17_17275	D2_contig_29_10	hypothetical protein
7	A5N17_17280	D2_contig_29_11	MFS transporter
8	A5N17_17285	D2_contig_29_12	glyoxalase
9	A5N17_17290	D2_contig_29_13	oxidoreductase
10	A5N17_17295	D2_contig_29_14	aryl acylamidase
11	A5N17_17300	D2_contig_29_15	ABC transporter substrate-binding protein
12	A5N17_17305	D2_contig_29_16	ABCtransporterATP-bindingprotein
13	A5N17_17310	D2_contig_29_17	ABCtransporterATP-bindingprotein
14	A5N17_17315	D2_contig_29_18	ABCtransporter permease
15	A5N17_17320	D2_contig_29_19	ABC transporter permease
16	A5N17_17325	D2_contig_29_20	esterase
17	A5N17_17330	D2_contig_29_21	hypotheticalprotein
18	A5N17_17335	D2_contig_29_23	hypotheticalprotein
19	A5N17_17340	D2_contig_29_24	hypotheticalprotein
20	A5N17_17345	D2_contig_29_25	oxidoreductase
21	A5N17_17350	D2_contig_29_26	aminopeptidase
22	A5N17_17355	D2_contig_29_27	hypotheticalprotein
23	A5N17_17360	D2_contig_29_28	chromosome partitioning protein ParA
24	A5N17_17365	D2_contig_29_30	hypotheticalprotein
25	A5N17_17370	D2_contig_29_31	hypotheticalprotein
26	A5N17_17375	D2_contig_29_32	NrdH-redoxin
27	A5N17_17380	D2_contig_29_33	hypotheticalprotein
28	A5N17_17385	D2_contig_29_34	hypotheticalprotein
29	A5N17_17390	D2_contig_29_35	hypothetical protein
30	A5N17_17395	D2_contig_29_36	plasmid partitioning protein
31	A5N17_17400	D2_contig_29_37	Yag1E
32	A5N17_17405	D2_contig_29_38	hypothetical protein
33	A5N17_17410	D2_contig_29_39	DNA methyltransferase
34	A5N17_17415	D2_contig_29_40	hypothetical protein
35	A5N17_17420	D2_contig_29_41	hypothetical protein

36	A5N17_17425	D2_contig_29_42	hypothetical protein
37	A5N17_17430	D2_contig_29_43	hypothetical protein
38	A5N17_17435	D2_contig_29_44	hypothetical protein
39	A5N17_17440	D2_contig_29_45	hypothetical protein
40	A5N17_17445	D2_contig_29_46	hypothetical protein

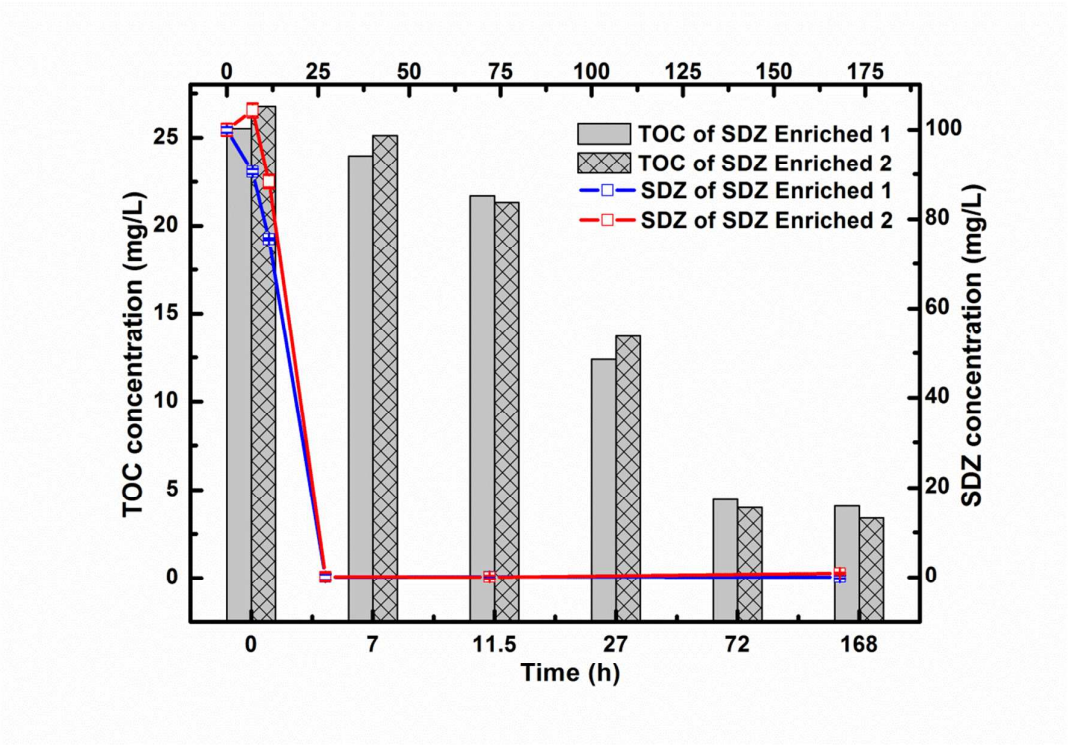

Figure S1. Degradation of SDZ and TOC mineralization by enriched consortia.

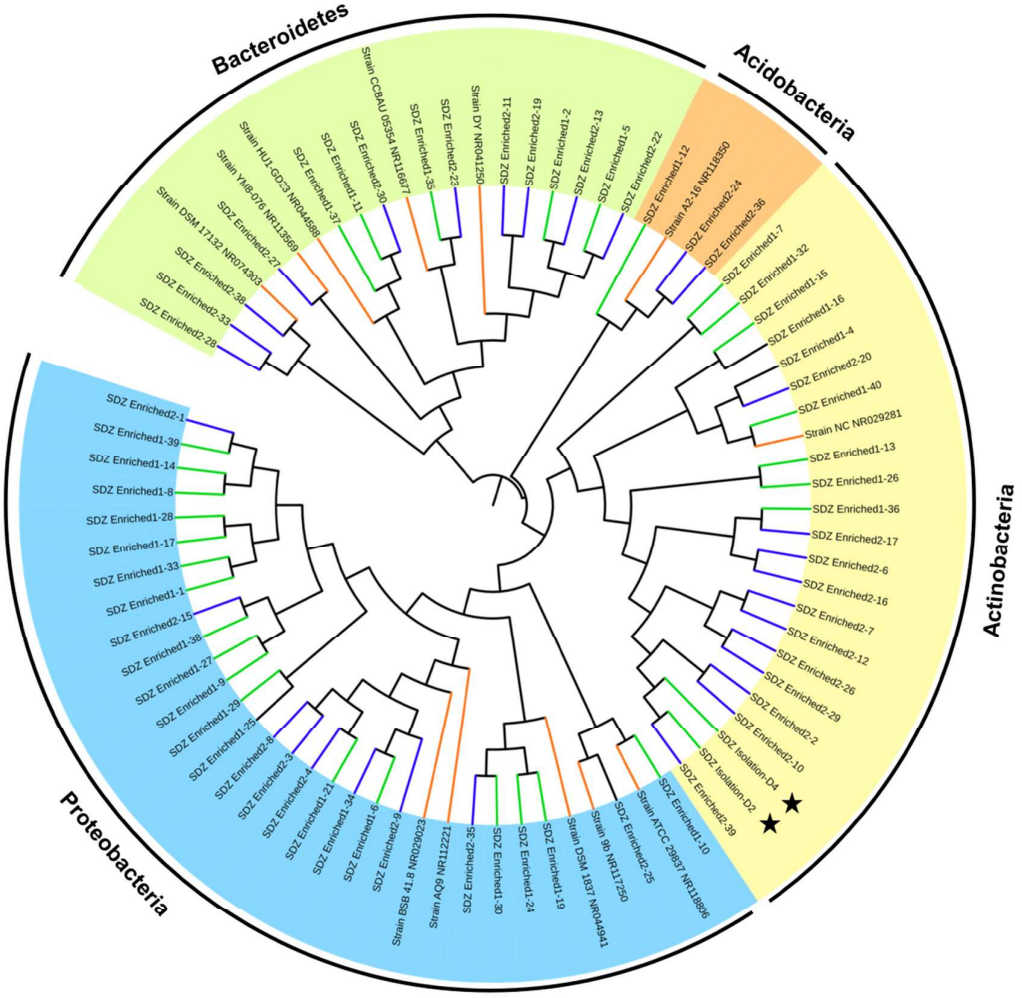

Figure S2. Overall microbial community for two SDZ-enriched consortia. Leaf branch color represents the sources of the clones (Green for SDZ Enriched 1, blue for SDZ Enriched 2 and orange for reference sequences); Leaf label color represents the taxonomy and label with star represents the isolate.

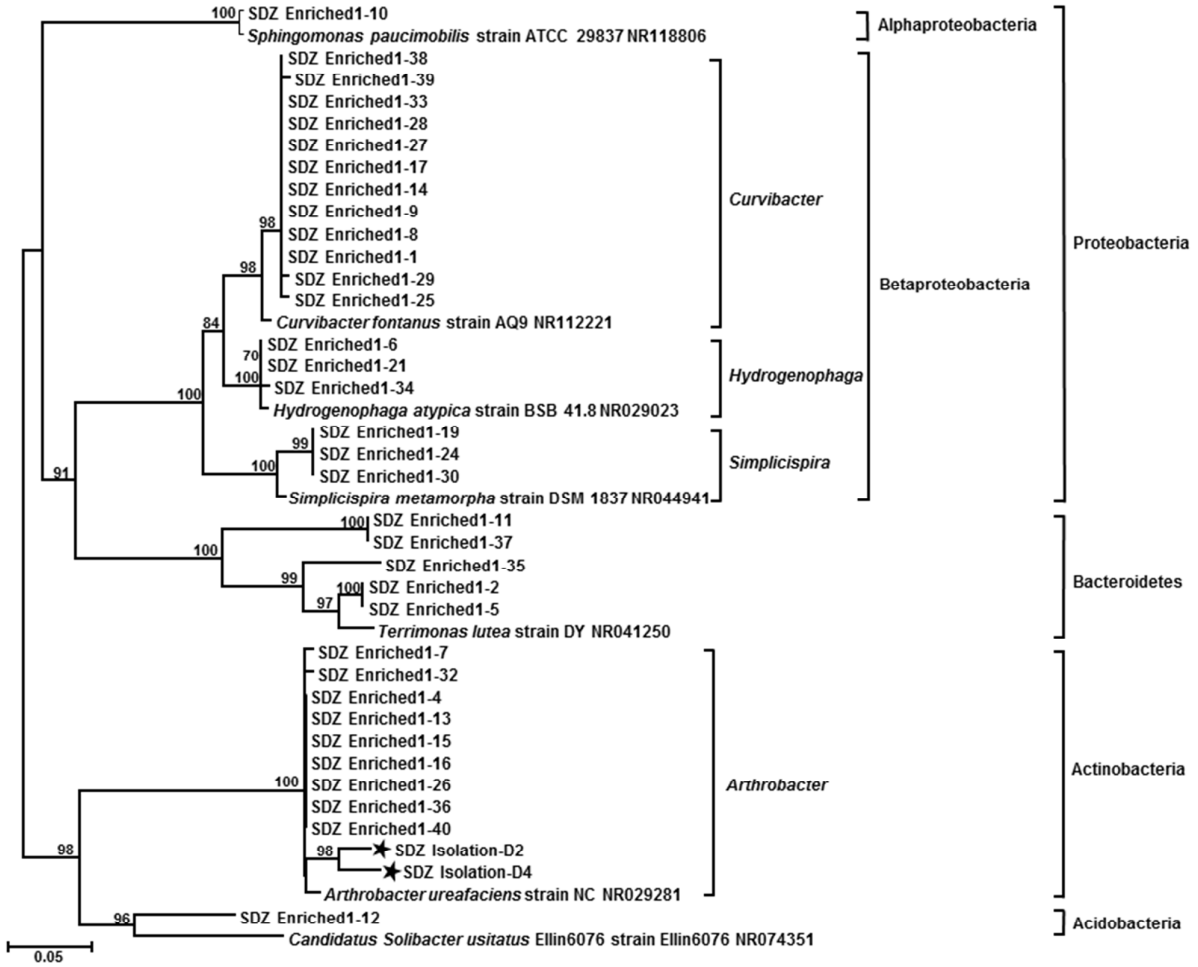

Figure S3. Phylogenetic tree of reactor SDZ Enriched 1 and two isolates.

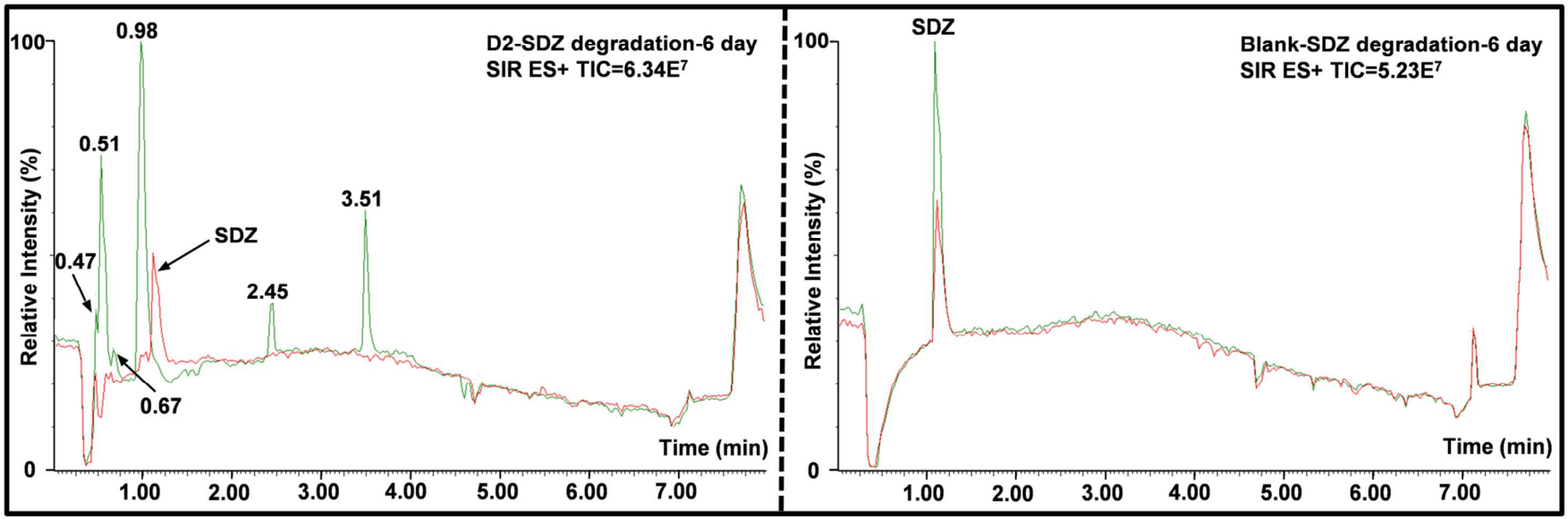

Figure S4. Total chromatographic profile of the putative biodegradtion products generated from non-target screening (full-scan MS mode). The SIR total chromatography for t=6 day sample (green line) was overlaid on that for t=0 sample (red line). Initially, a list of 28 putative biodegradation products was included in this total chromatography by Selected Ion Recording (SIR) mode. False positives subtraction was subsequently conducted by filtering these 28 masses based on quantitative assessment from Multiple Reaction Monitoring (MRM) mode (see detailed list and filtering processes in the Table S5).

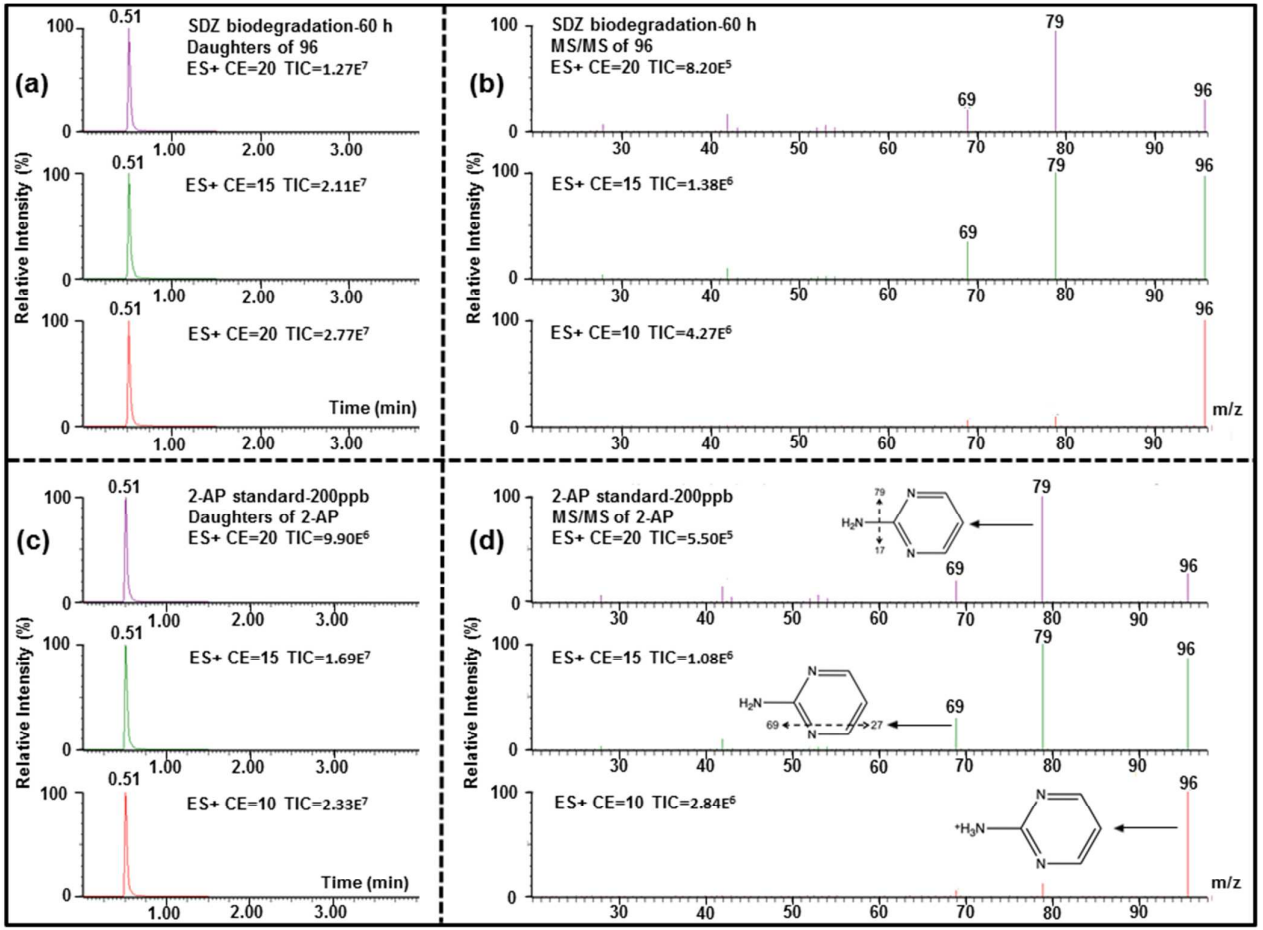

Figure S5. Analytical data for detected ion at *m/z* 96 including (a) chromatogram of the ion at *m/z* 96; (b) MS/MS spectrum of the ion at *m/z* 96; (c) chromatogram of the reference standard 2-aminopyrimidine; (d) MS/MS spectrum of the reference standard 2-aminopyrimidine.

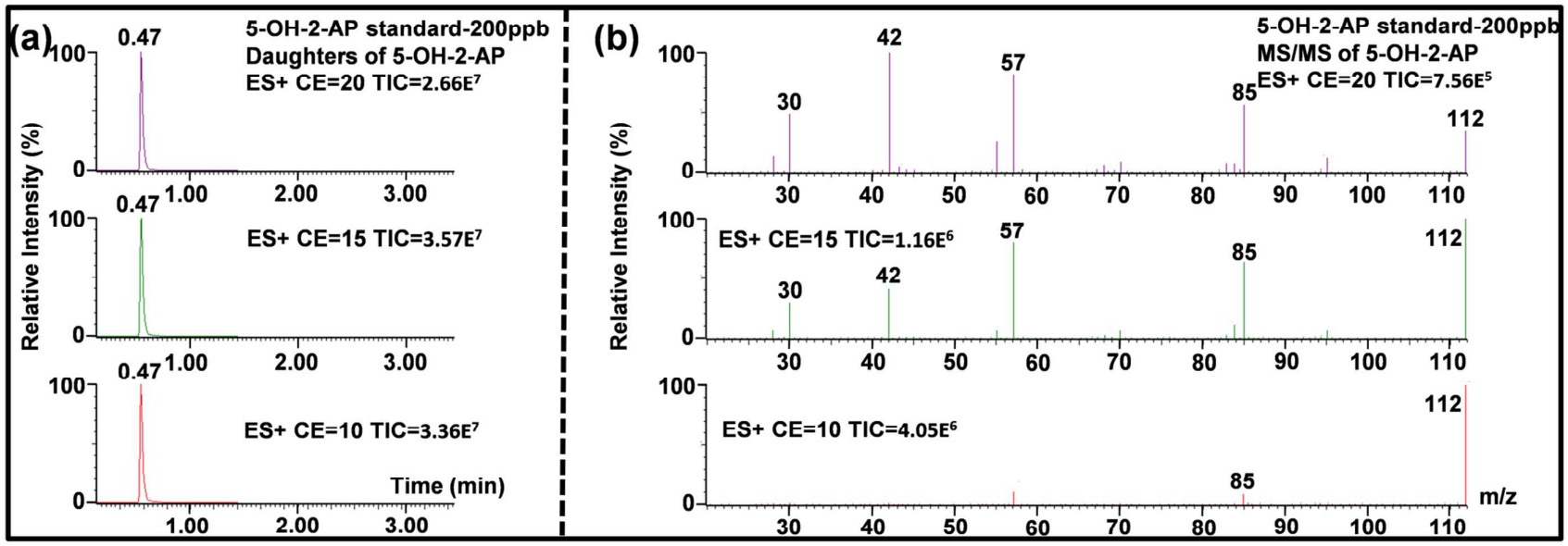

Figure S6. Analytical data for 2-amino-5-hydroxpyrimidine including (a) chromatogram of 5-OH-2-AP; (b) MS/MS spectrum of 5-OH-2-AP.

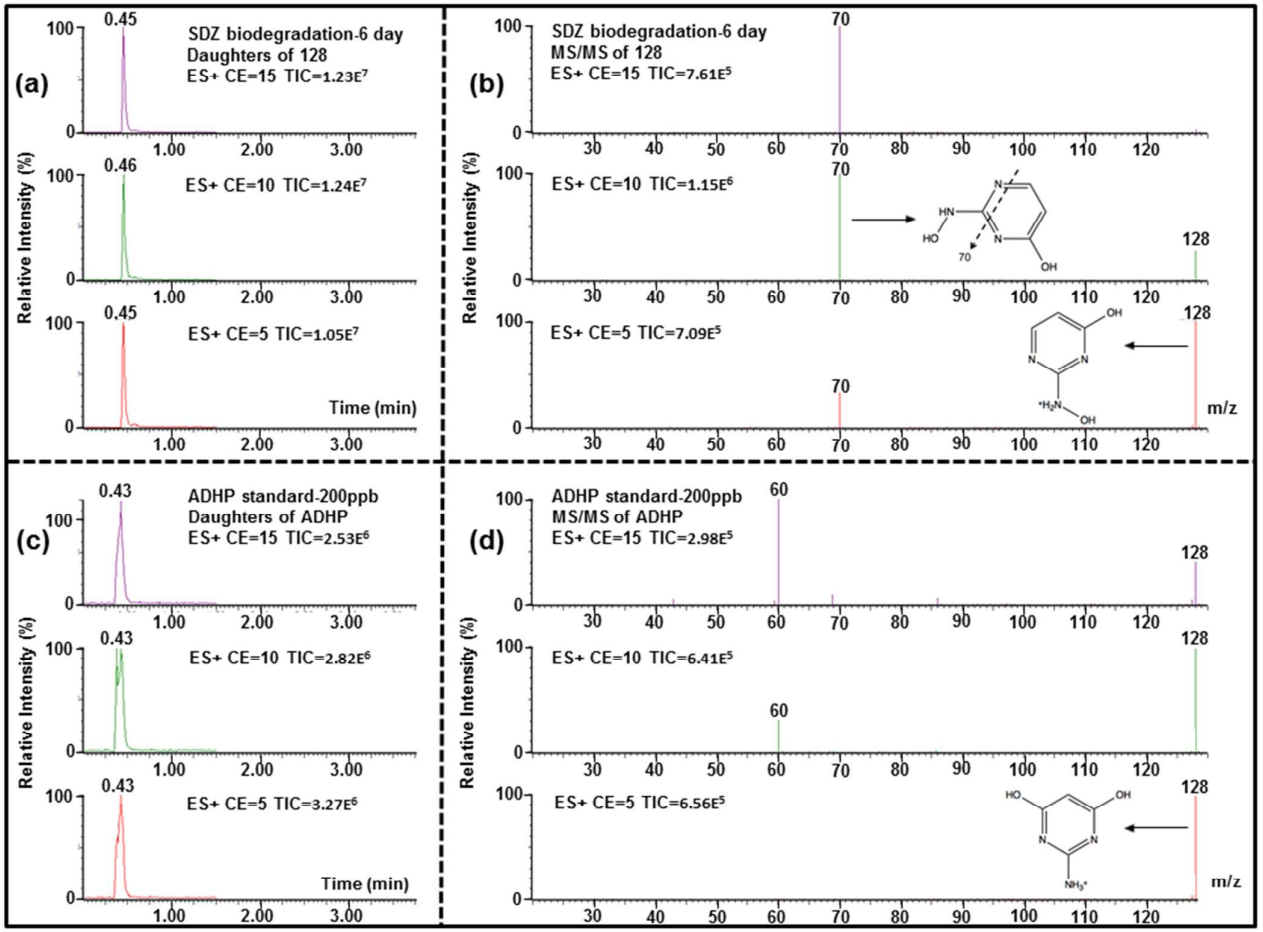

Figure S7. Analytical data for detected ion at *m/z* 128 including (a) chromatogram of the ion at *m/z* 128; (b) MS/MS spectrum of the ion at *m/z* 128; (c) chromatogram of the reference standard 2-amino-4, 6-dihydroxypyrimidine (ADHP); (d) MS/MS spectrum of the reference standard.

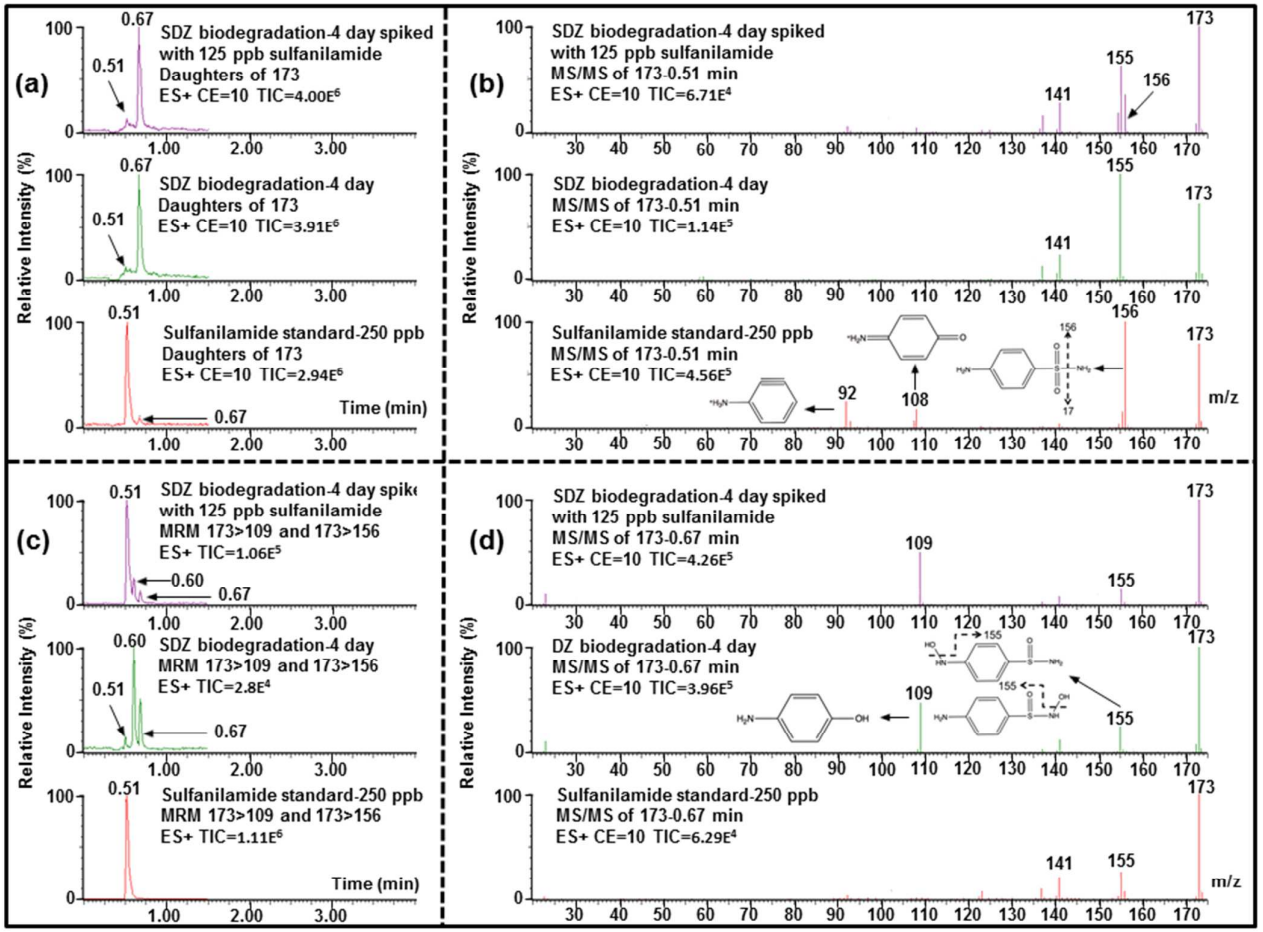

Figure S8. Analytical data for detected ion at *m/z* 173including (a) chromatogram of the detected ion at *m/z* 173 ; (b) MS/MS spectrum of the peak at 0.51 min; (c) MRM detection of characteristic fragment ions at *m/z* 109 and 156; (d) MS/MS spectrum of the peak at 0.67 min.

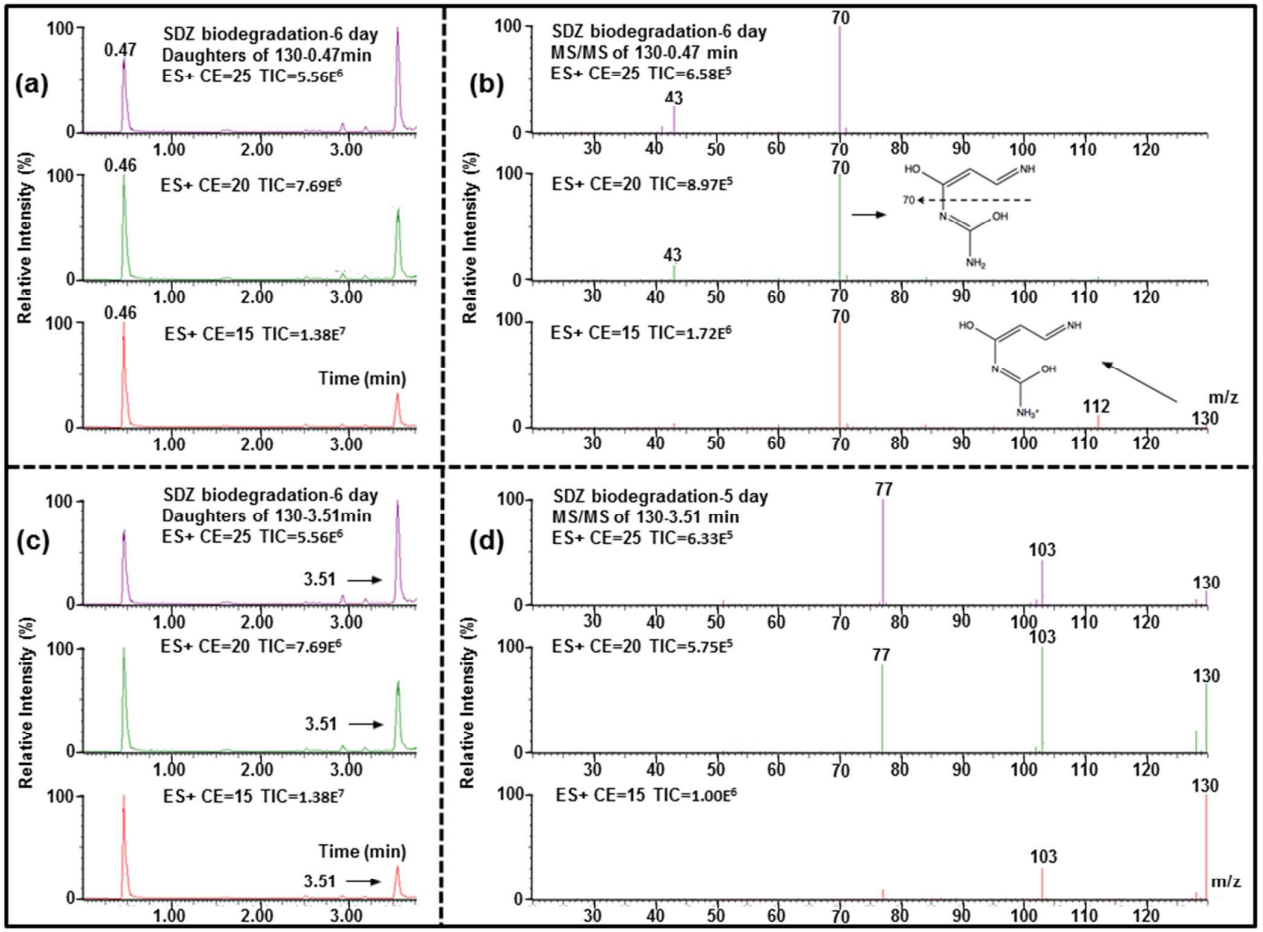

Figure S9. Analytical data for detected ion at *m/z* 130 including (a) chromatogram of the ion at m/z 130 eluted at 0.47 min; (b) MS/MS spectrum of the peak at 0.47 min; (c) chromatogram of the the ion at m/z 130 eluted at 3.51min; (d) MS/MS spectrum of the peak at 3.51 min.

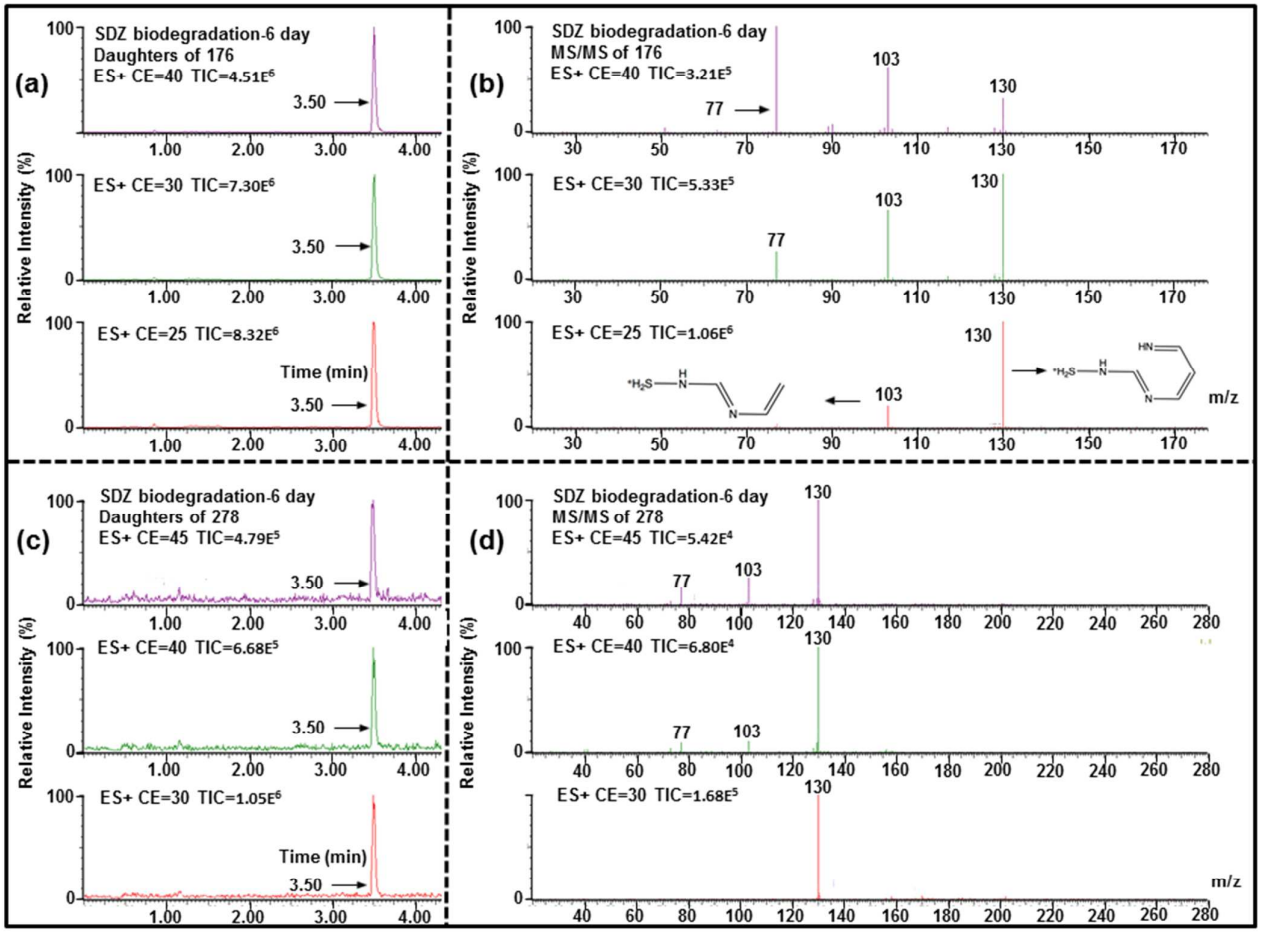

Figure S10. Analytical data for detected ion at *m/z* 176 and 278 including (a) chromatogram of the ion at m/z 176; (b) MS/MS spectrum of the ion at m/z 176; (c) chromatogram of the ion at m/z 278; (d) MS/MS spectrum of the ion at m/z 278.

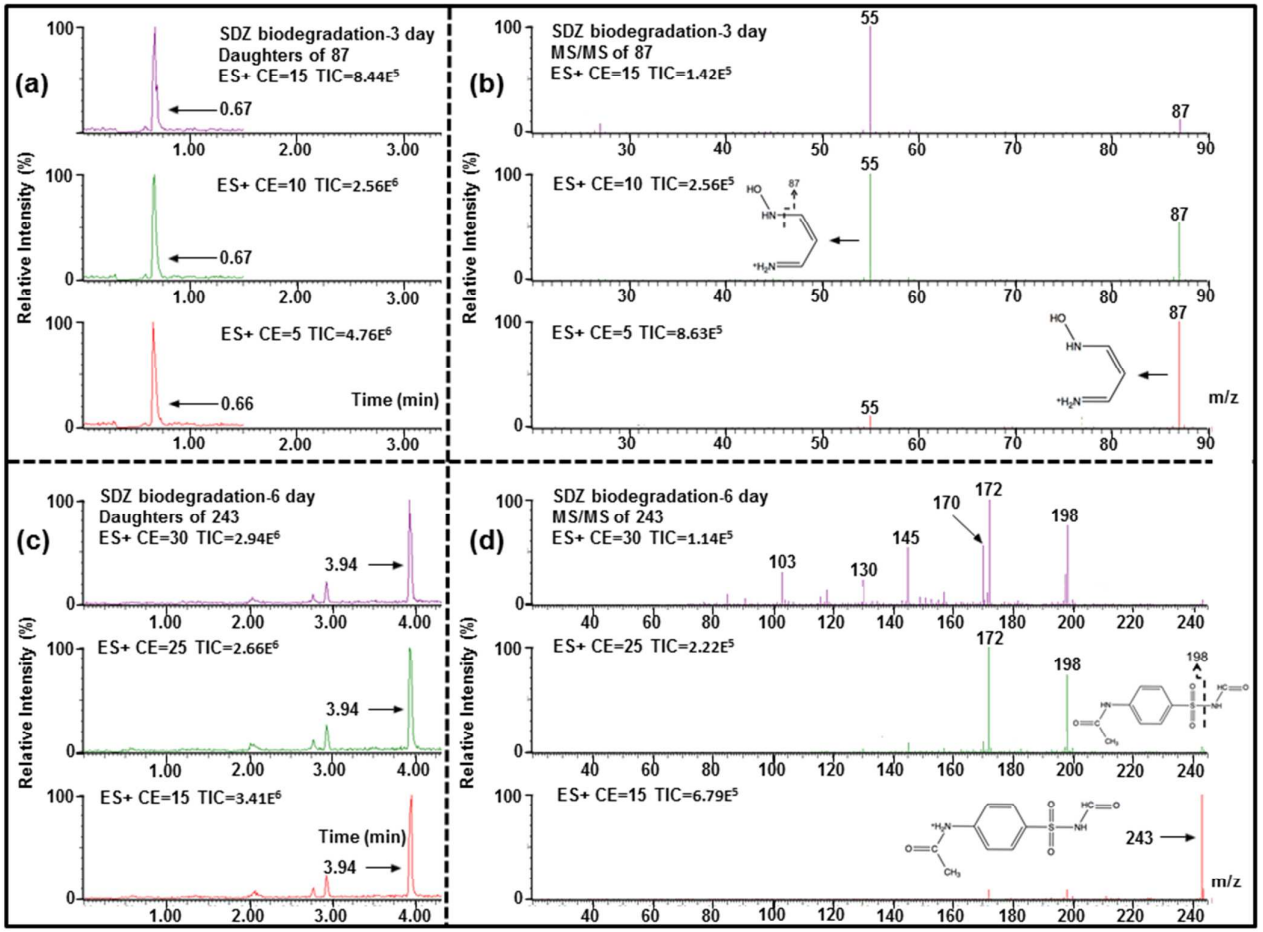

Figure S11. Analytical data for detected ion at *m/z* 87 and 243 including (a) chromatogram of the ion at m/z 87; (b) MS/MS spectrum of the ion at m/z 87; (c) chromatogram of the ion at m/z 243; (d) MS/MS spectrum of the ion at m/z 243.

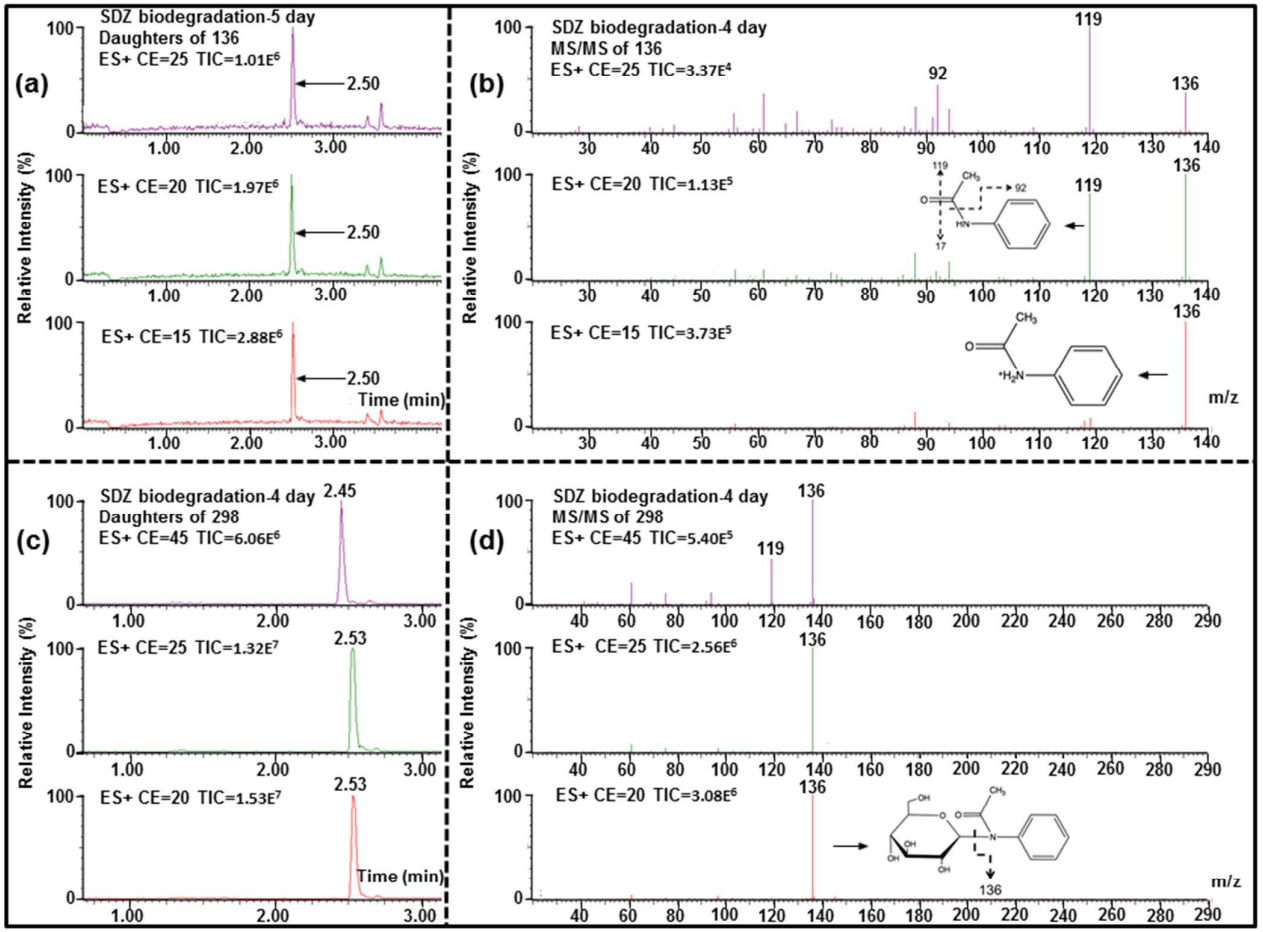

Figure S12. Analytical data for detected ion at *m/z* 136 and 298 including (a) chromatogram of the ion at m/z 136; (b) MS/MS spectrum of the ion at m/z 136; (c) chromatogram of the ion at m/z 298; (d) MS/MS spectrum of the ion at m/z 298.

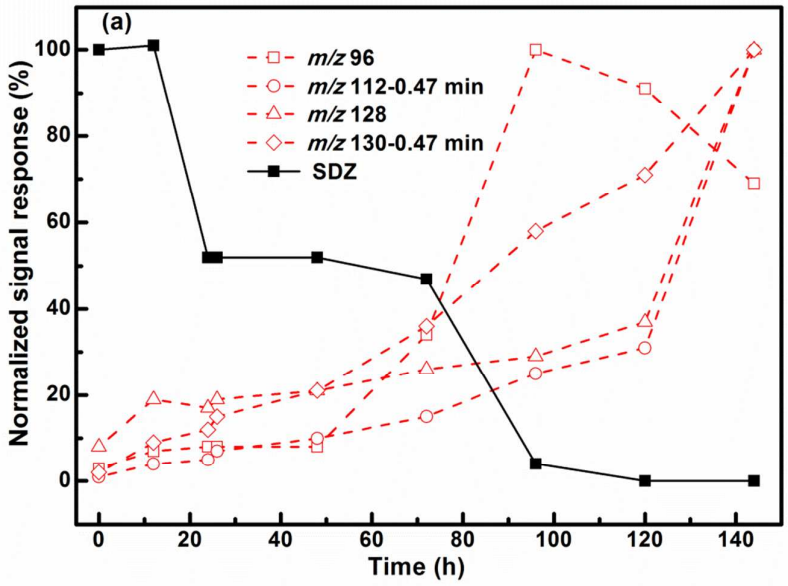
(a)
m/z 96
m/z 112-0.47 min
m/z 128
m/z 130-0.47 min
SDZ
Normalized signal response (%)
Time (h)
0
20
40
60
80
100
120
140

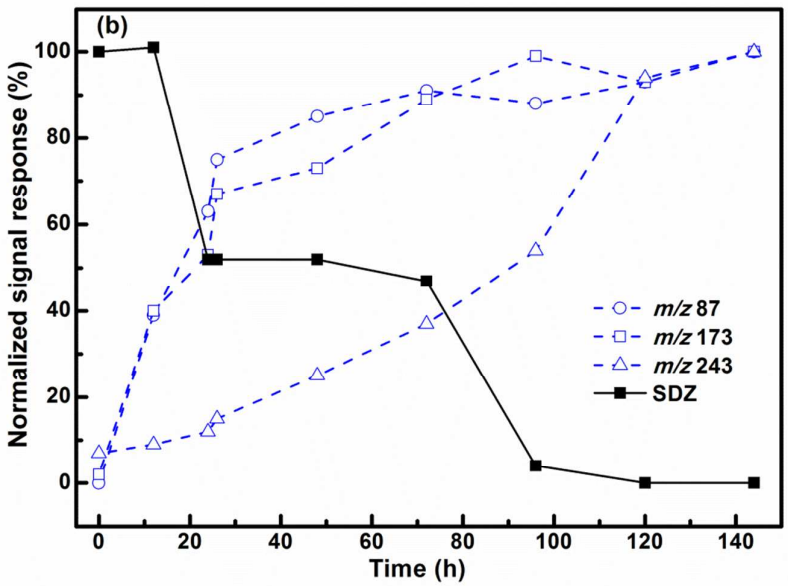
(b)
m/z 87
m/z 173
m/z 243
SDZ
Normalized signal response (%)
Time (h)
0
20
40
60
80
100
120
140

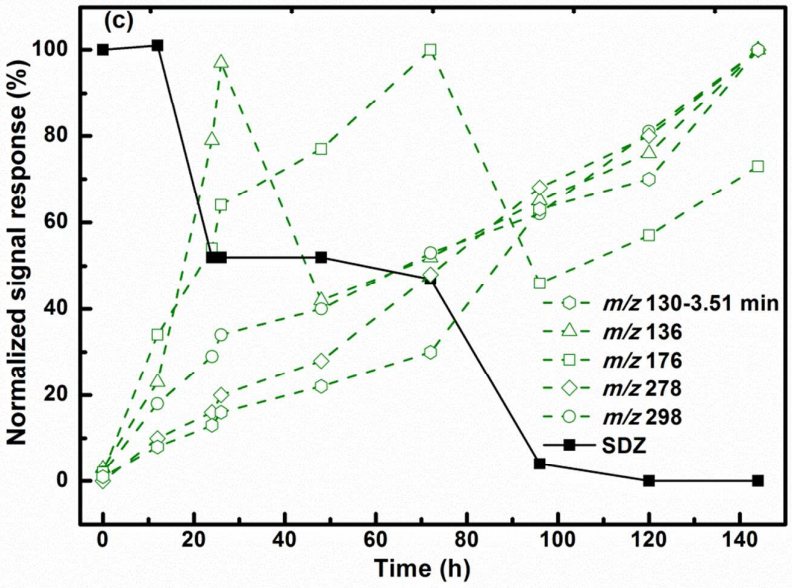
(c)
Normalized signal response (%)
Time (h)
m/z 130-3.51 min
m/z 136
m/z 176
m/z 278
m/z 298
SDZ

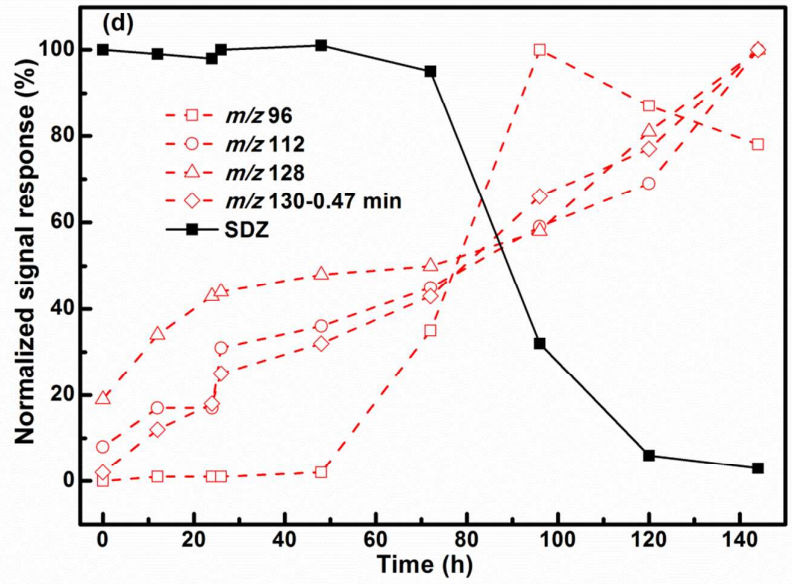
(d)
Normalized signal response (%)
Time (h)
m/z 96
m/z 112
m/z 128
m/z 130-0.47 min
SDZ

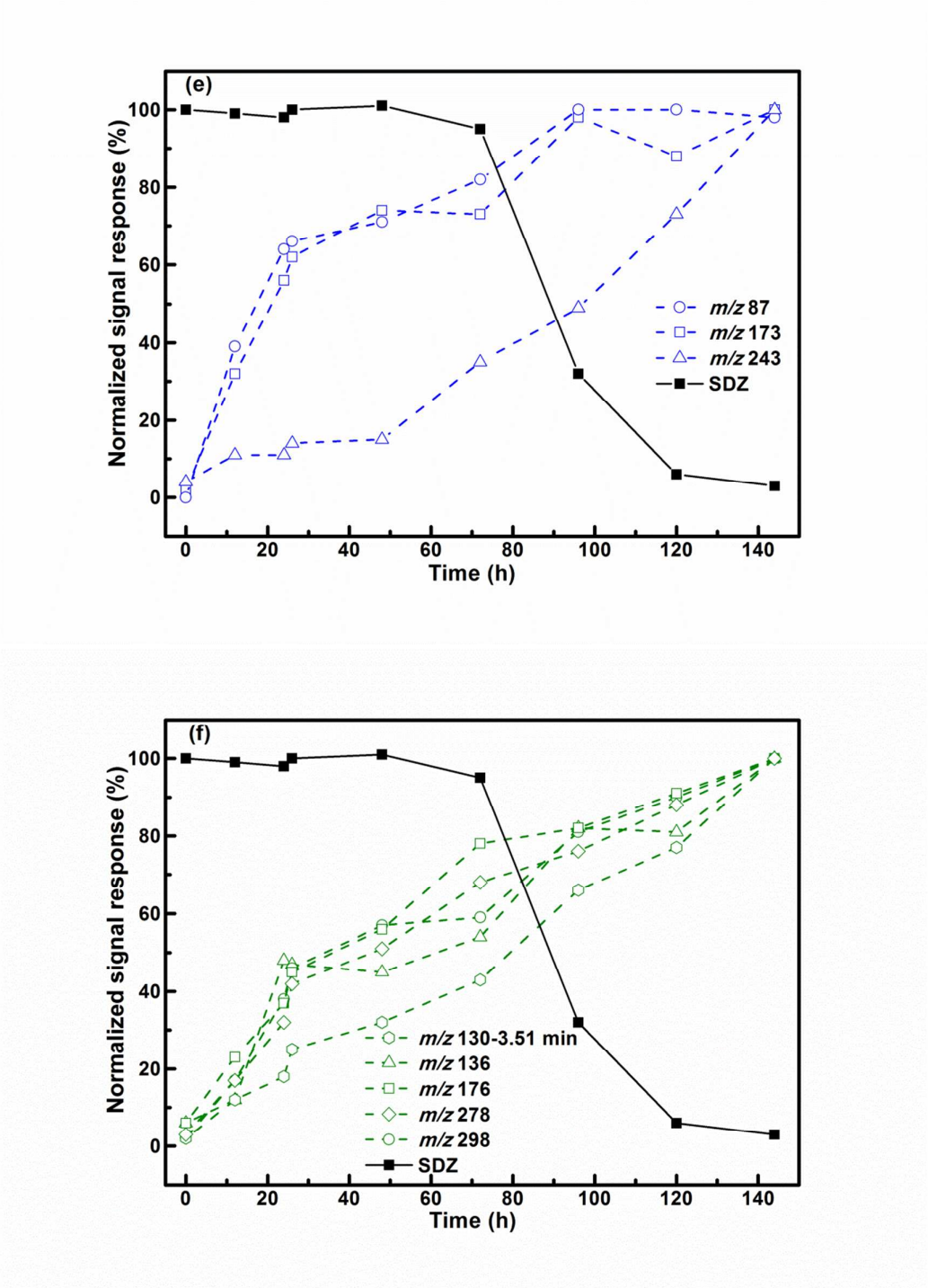

Figure S13. Time courses of SDZ degradation by strain D2 (a-c) and D4 (d-f) and their proposed products formation (Red line represents pathway I; blue line represents pathway II; green line represents pathway III). Time series patterns were plotted as the signal response changes in a function of time. The signal responses were normalized as a ratio of their measured chromatographic areas at a specific time to that at time zero.

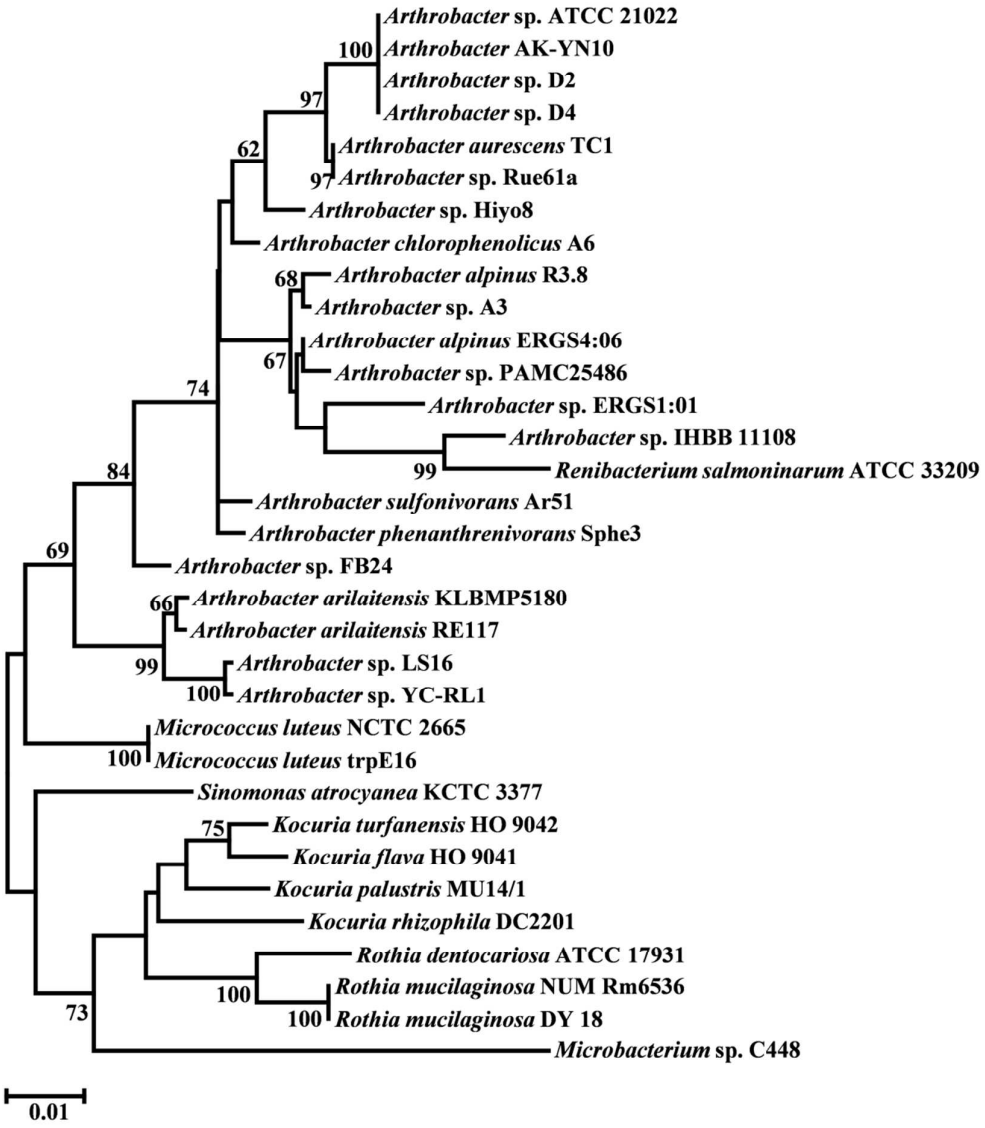

Figure S14. Maximum likelihood tree of isolates D2 and D4 in the context of all the 29 finished genomes in genus *Arthrobacter* and two draft genomes of *Arthrobacter* sp. AK-YN10 and *Microbacterium* sp. C448 using 16S rRNA genes. Bootstrap values were supported by 1000 replications and the value lower than 60% were not shown. The scale bar represents 1% estimated sequence divergence

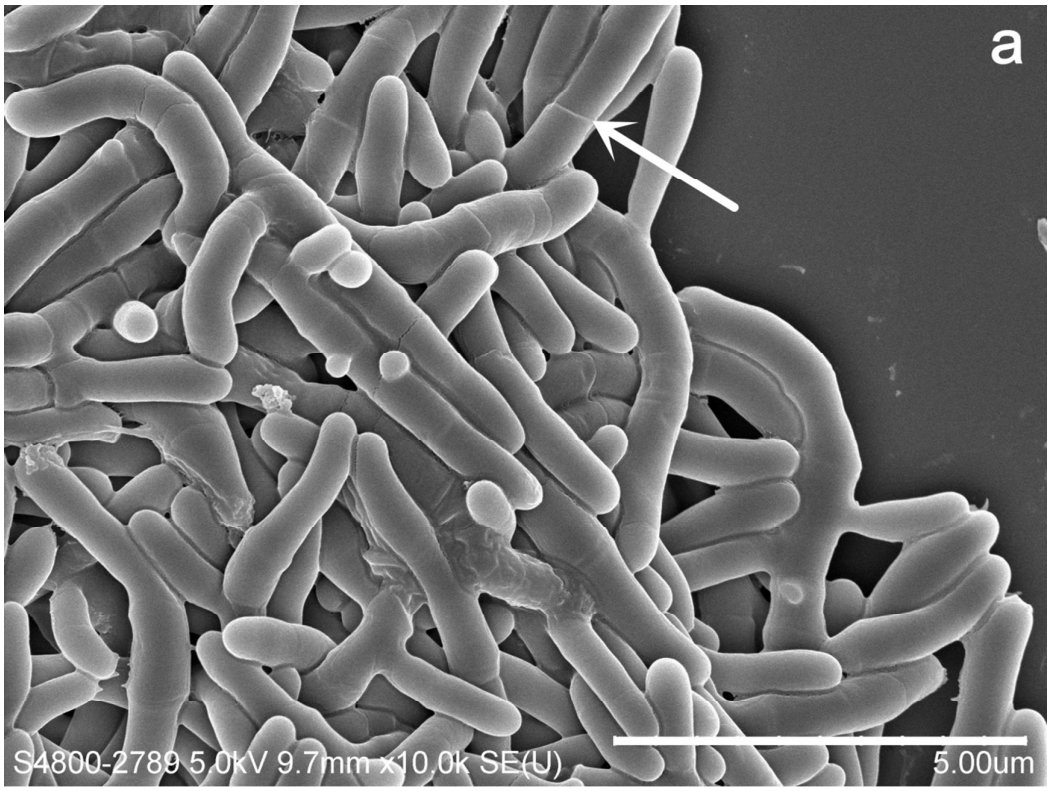
a
S4800-2789 5.0kV 9.7mm x10.0k SE(U)
5.00um

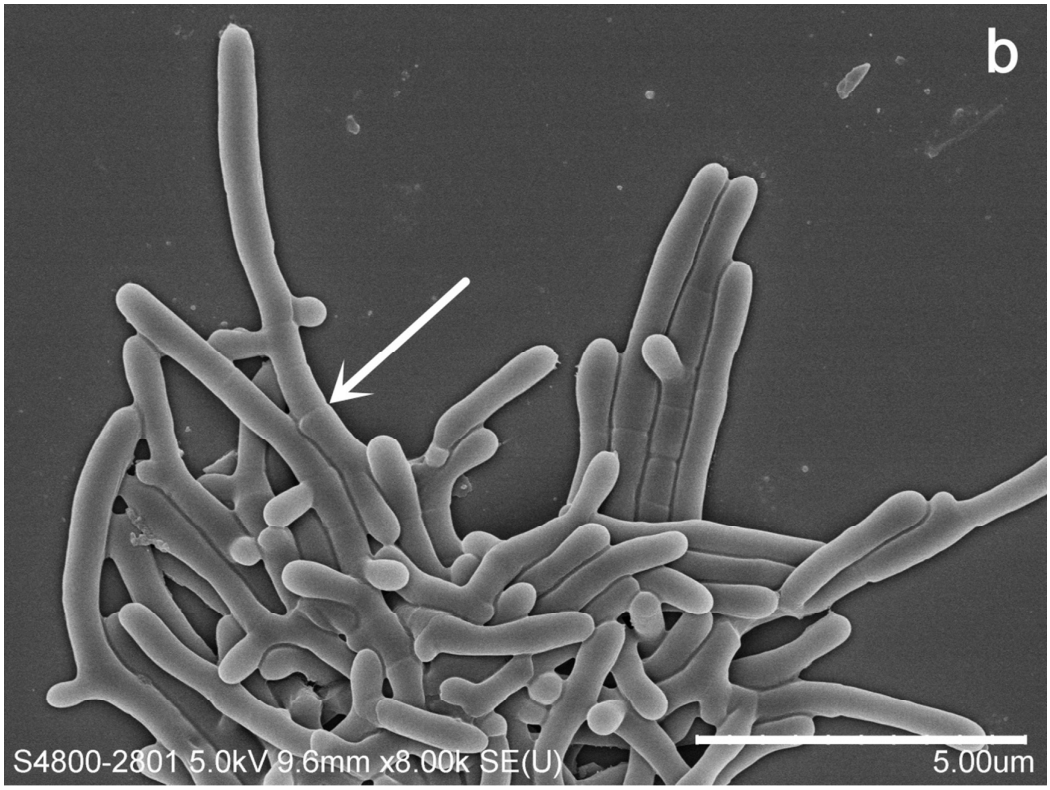
b
S4800-2801 5.0kV 9.6mm x8.00k SE(U)
5.00um

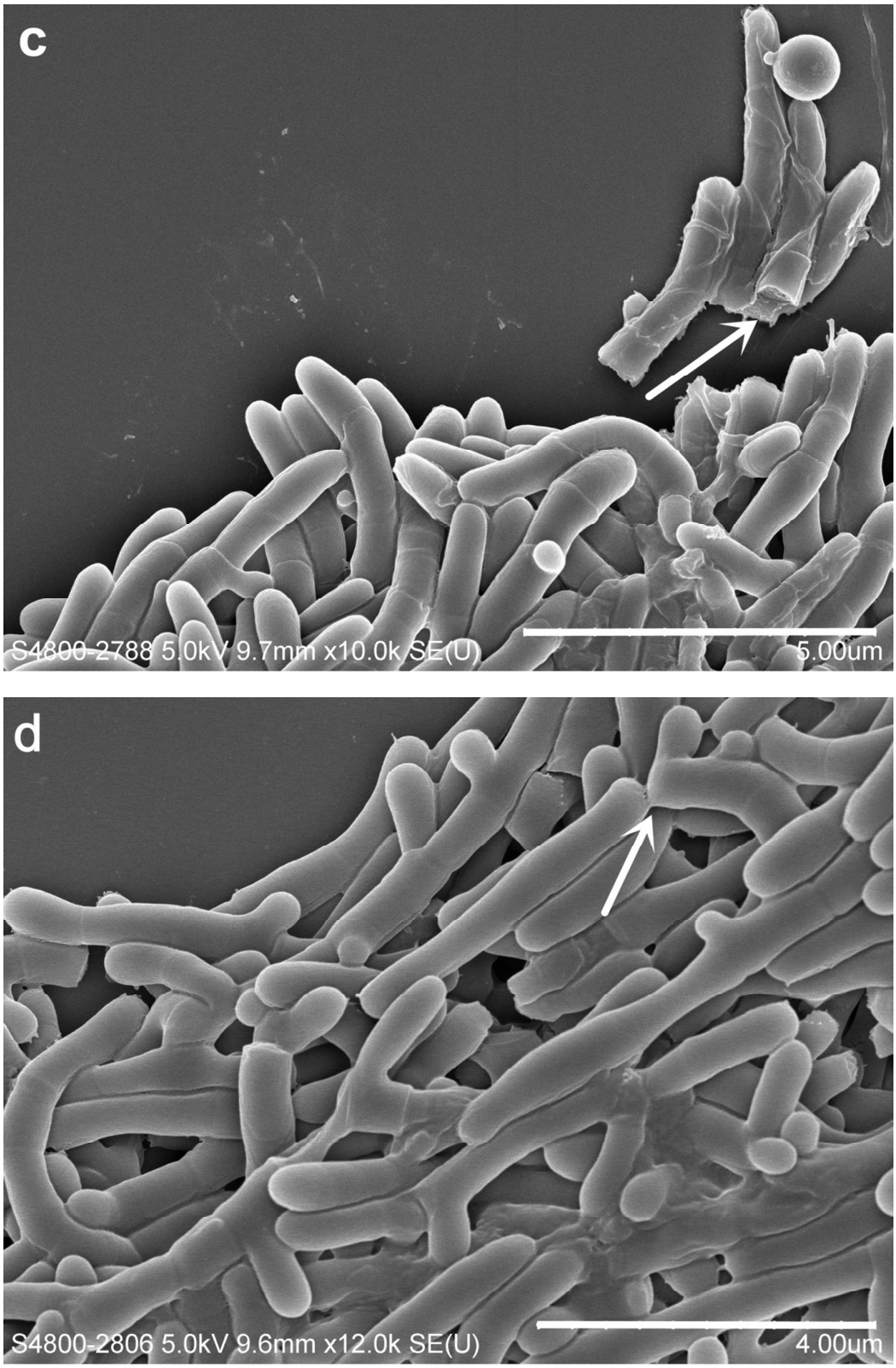

Figure S15. Scanning electron microscope (SEM) images of D2 (a and c) and D4 (b and d).

REFERENCES

1. Schleifer, K. H.; Kandler, O., Peptidoglycan types of bacterial cell walls and their taxonomic implications. *Bacteriological reviews* **1972,** *36*, (4), 407.
2. Reddy, G.; Aggarwal, R.; Matsumoto, G.; Shivaji, S., Arthrobacter flavus sp. nov., a psychrophilic bacterium isolated from a pond in McMurdo Dry Valley, Antarctica. *International journal of systematic and evolutionary microbiology* **2000,** *50*, (4), 1553-1561.
3. Krulwich, T. A.; Pate, J. L., Ultrastructural explanation for snapping postfission movements in Arthrobacter crystallopoietes. *Journal of bacteriology* **1971,** *105*, (1), 408-412.
4. Loveland-Curtze, J.; Sheridan, P. P.; Gutshall, K. R.; Brenchley, J. E., Biochemical and phylogenetic analyses of psychrophilic isolates belonging to the Arthrobacter subgroup and description of Arthrobacter psychrolactophilus, sp. nov. *Archives of microbiology* **1999,** *171*, (6), 355-363.
5. KOMAGATA, K.; YAMADA, K.; OGAWA, H., TAXONOMIC STUDIES ON CORYNEFORM BACTERIA. *The Journal of General and Applied Microbiology* **1969,** *15*, (3), 243-259.
6. Dahl, J. L., Electron microscopy analysis of Mycobacterium tuberculosis cell division. *FEMS microbiology letters* **2004,** *240*, (1), 15-20.
7. Majewsky, M.; Glauner, T.; Horn, H., Systematic suspect screening and identification of sulfonamide antibiotic transformation products in the aquatic environment. *Analytical and bioanalytical chemistry* **2015,** *407*, (19), 5707-5717.
8. Vree, T.; Van der Ven, A.; Verwey-van Wissen, C.; Kolmer, E. v. E.-B.; Swolfs, A.; Van Galen, P.; Amatdjais-Groenen, H., Isolation, identification and determination of sulfamethoxazole and its known metabolites in human plasma and urine by high-performance liquid chromatography. *Journal of Chromatography B: Biomedical Sciences and Applications* **1994,** *658*, (2), 327-340.
9. García-Galán, M. J.; Rodríguez-Rodríguez, C. E.; Vicent, T.; Caminal, G.; Díaz-Cruz, M. S.; Barceló, D., Biodegradation of sulfamethazine by Trametes versicolor: Removal from sewage sludge and identification of intermediate products by UPLC–QqTOF-MS. *Science of the total environment* **2011,** *409*, (24), 5505-5512.
10. Wang, J.; Gardinali, P. R., Identification of phase II pharmaceutical metabolites in reclaimed water using high resolution benchtop Orbitrap mass spectrometry. *Chemosphere* **2014,** *107*, 65-73.